# Supporting Information

## Crowe et al. 10.1073/pnas.1717015115

### Characterization of Metabolites

**COCHEA-CoA.** $C_{32}H_{49}N_7O_{20}P_3S^+$ predicted $[M + H]^+ = 976.1960$; electrospray ionization (ESI)-MS: $[M + H]^+ = 976.1974$ (1.4 ppm from prediction).

$$\lambda_{max} = 252\text{nm}\left(\varepsilon_{252} = 17.2\ \text{mM}^{-1}\cdot\text{cm}^{-1}\right)$$

**MOODA-CoA.** $C_{30}H_{49}N_7O_{20}P_3S^+$ predicted $[M + H]^+ = 952.1970$; ESI-MS: $[M + H]^+ = 952.1989$ (2.4 ppm from prediction).

$$\lambda_{max} = 258\ \text{nm}\left(\varepsilon_{258} = 11.9\ \text{mM}^{-1}\cdot\text{cm}^{-1},\ \varepsilon_{252} = 10.4\ \text{mM}^{-1}\cdot\text{cm}^{-1}\right)$$

$^1$H-NMR (600 MHz, $D_2O$): δ(ppm) = 8.53 (s, 1H), 8.24 (s, 1H), 6.2 (d, 1H), 4.65 (s, 1H), 4.2 (s, 2H), 4.0 (s, 2H), 3.8 (m, 1H), 3.6–3.5 (m, 2H), 3.50 (q, 2H), 3.49 (m, 3H), 3.30–3.45 (m, 4H), 2.95 (q, 2H), 2.83 (m, 1H), 2.73 (m, 1H), 2.68 (m, 1H), 2.58 (q, 2H), 2.3–2.4 (m, 4H), 1.64 (m, 1H), 1.05 (d, 3H), 0.86 (s, 3H), 0.72 (s, 3H).

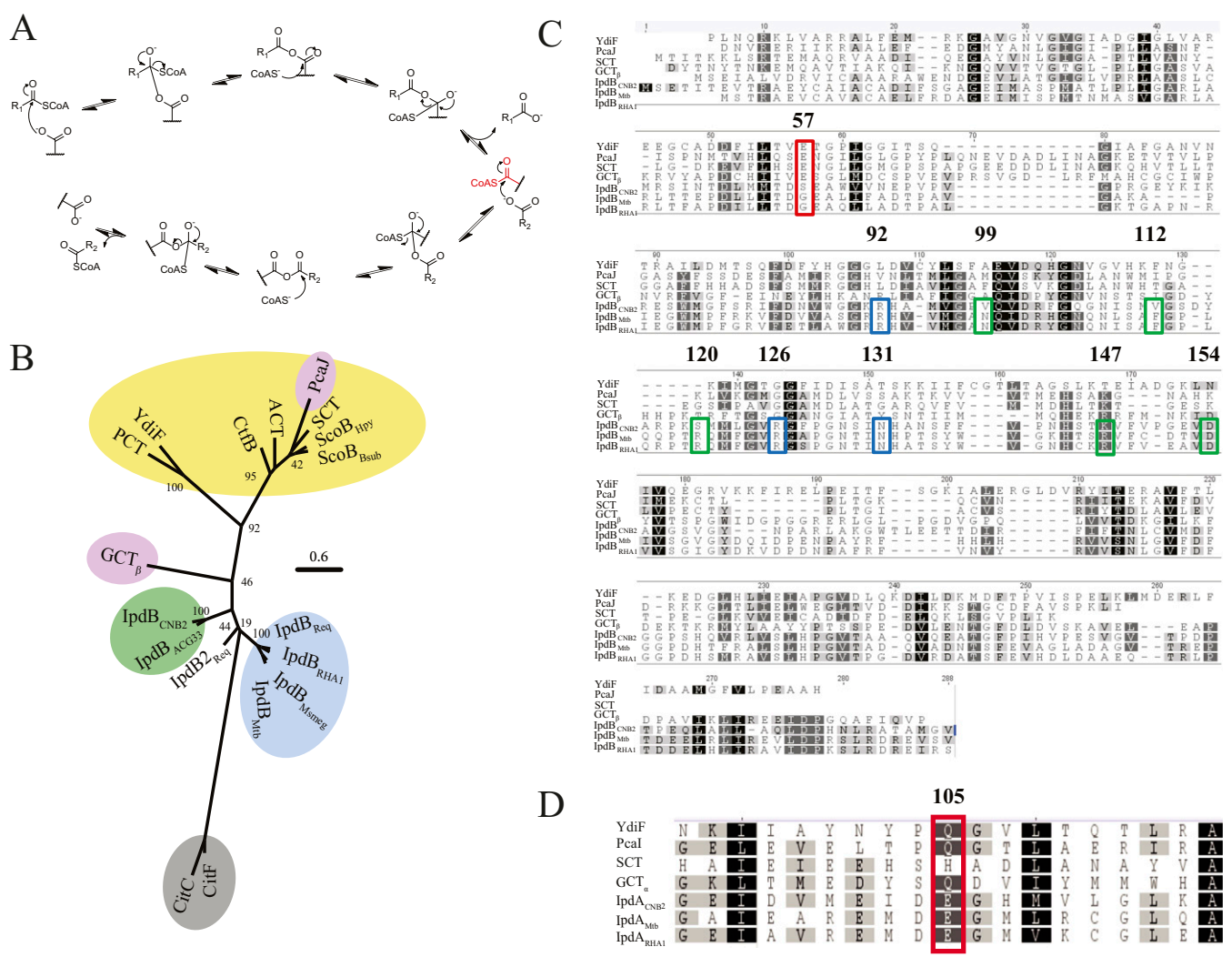


**Fig. S1.** Additional bioinformatic analysis of IpdAB and CoTs. (*A*) Conserved ping-pong mechanism of class I CoTs. The species in red represents the glutamyl-CoA intermediate. (*B*) Bioinformatic analysis of IpdAB and homologs. Phylogenetic tree displaying IpdB and β-subunits from class I and II CoTs. Shaded regions indicate gram-positive IpdB (blue), gram-negative IpdB (green), or class I β-keto-CoA (purple), class I (yellow), and class II (gray) CoTs. Proteins displayed are IpdB from *R. jostii* RHA1 ($IpdB_{RHA1}$), *R. equi* ($IpdB_{Req}$; $IpdB2_{Req}$), *M. smegmatis* ($IpdB_{Msmeg}$), *Mtb* ($IpdB_{Mtb}$), *S. denitrificans* ($IpdB_{ACG33}$), and *C. testosteroni CNB-2* ($IpdB_{CNB-2}$); β-ketoadipyl-CoT from *P. putida* (PcaJ); glutaconate CoT from *A. fermentans* (GCT), citrate lyases from *E. aerogenes* (CitC), and *C. argentinense* (CitF); butyrate-acetoacetate CoT from *C. acetobutylicum* (CtfB); acetate CoTs from *E. coli* (ACT and YdiF); succinyl-CoTs from *B. subtillus* ($ScoB_{Bsub}$), *H. pylori* ($ScoB_{Hpy}$), pig heart (SCT); and propionyl-CoT from *C. propionicum* (PCT). Additional information is available in *Supporting Information*. Numbers in the tree correspond to nonparametric bootstrap values from 100 maximum-likelihood calculations. (*B*) Amino acid alignment of IpdB (*C*) and IpdA (*D*) from CNB-2, *Mtb*, and RHA1 with well-characterized class I CoTs, YdiF, SCT, GCT, and PcaIJ. Red box indicates location of highly conserved catalytic glutamic acid in class I CoTs (*C*) or IpdA orthologs (*D*). Blue and green boxes indicate confirmed catalytic residues and CoA binding residues, respectively. Numbering corresponds to residue number in $IpdAB_{RHA1}$.

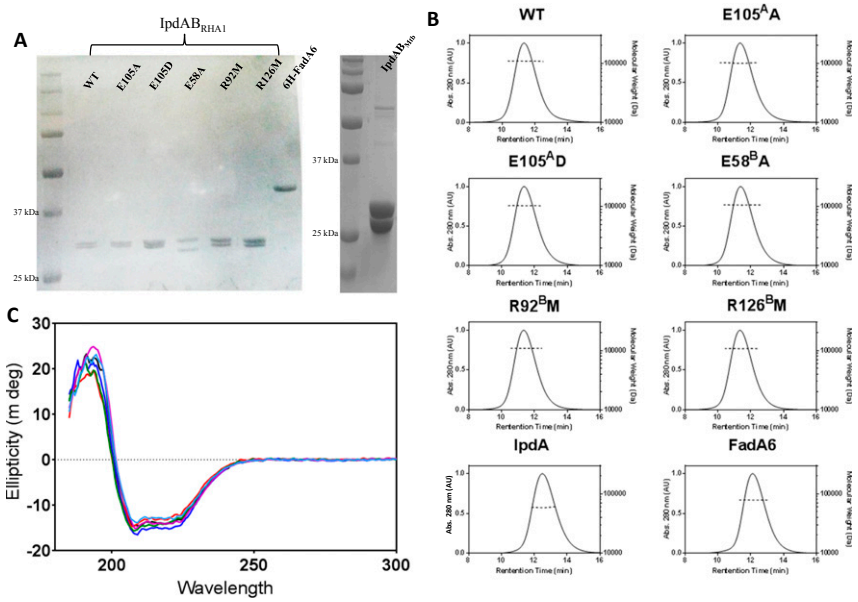


**Fig. S2.** Characterization of IpdAB. (*A*) SDS/PAGE showing ~1 μg of indicated protein. (*B*) SEC-MALS analysis of IpdAB and variants. Shown is the absorbance at 280 nm and the calculated molecular weight by the ASTRA6 software of proteins eluting from a Superdex 200 5/150 column. (*C*) CD spectra of 3 μM IpdAB (blue) or variants E105$^{A}$A (green), E105$^{A}$D (black), E58$^{B}$A (red), R126$^{B}$M (purple), and R92$^{B}$M (light blue) in 10 mM sodium phosphate, pH 8.0.

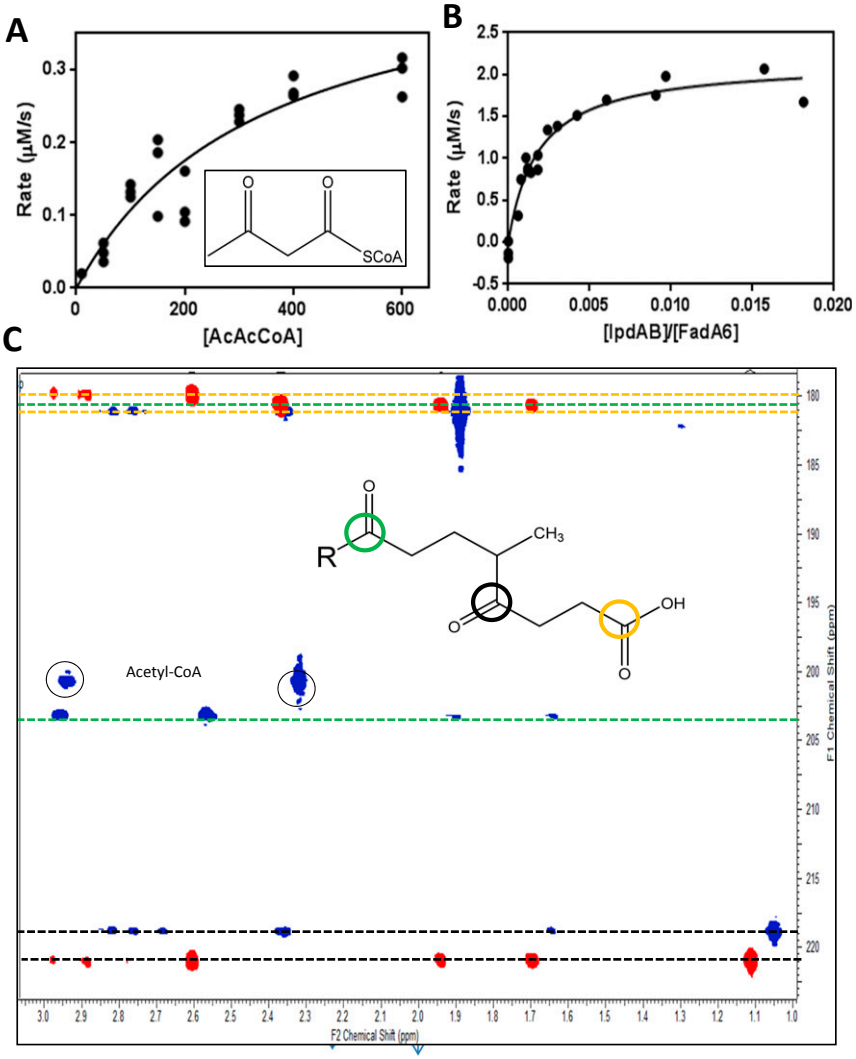


**Fig. S3.** FadA6 is a β-keto-CoA thiolase. (*A*) Steady-state kinetic analysis of FadA6 with acetoacetyl-CoA (*Inset*). Initial velocities were determined by monitoring the loss of absorbance at 310 nm due to thiolytic activity of the acetoacetyl-CoA-$Mg^{2+}$ enolate in Hepes, pH 7.5, and 10 mM $MgCl_2$ ($I = 0.05$ M). (*B*) Effect on the mole ratio between IpdAB and FadA6 on in vitro turnover of COCHEA-CoA to MOODA-CoA. Curves for *A* and *B* indicate best squares least fit of the Michaelis–Menten equation to the data as calculated by Origin. (*C*) The $^{1}H$-$^{13}C$ HMBC NMR spectra of MOODA-CoA (blue) and MOODA (red). Data were collected on a Bruker 600-MHz spectrophotometer using 1 mM MOODA-CoA dissolved in 400 μL $D_2O$. Shown is the 180–230 ppm region containing the carbonyl carbons identified in the *Inset*.

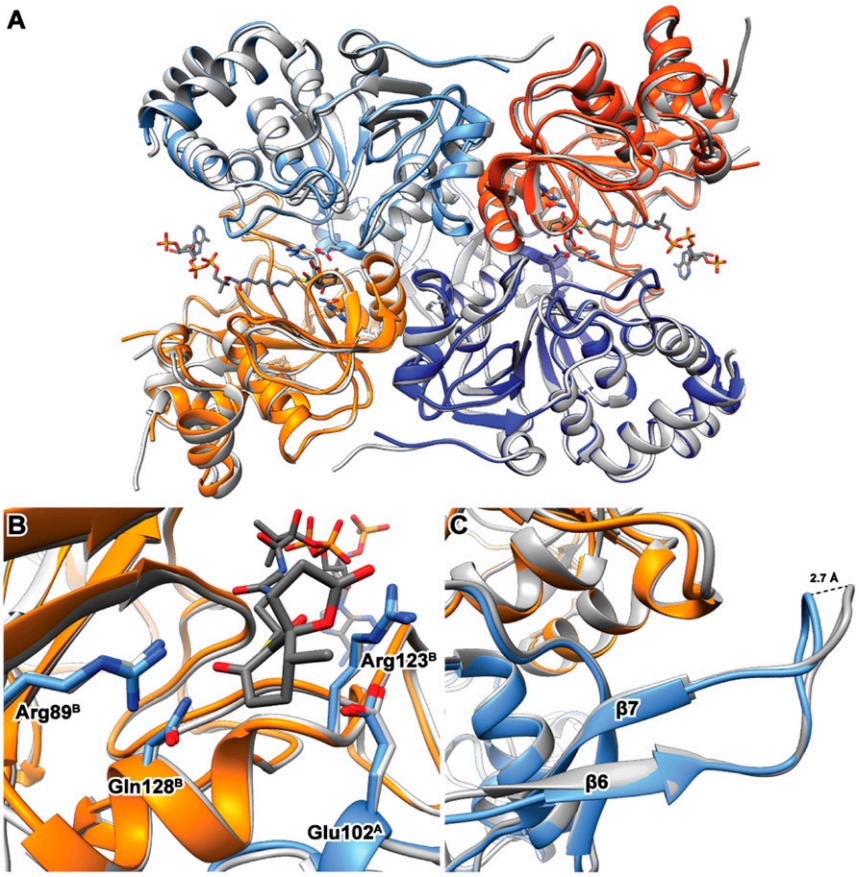


**Fig. S4.** Overlay of $IpdAB_{Mtb}$ and $IpdAB_{RHA1}$·COCHEA-CoA structures. (*A*) Superposition of the heterotetramers. (*B*) Overlay of the respective active sites and orientation of catalytic residues. (*C*) Conformational differences of the 10-residue loop between β-sheets 6 and 7. Distance measurement is from $C_\alpha$ of $IpdA_{Mtb}$. Coloring represents $IpdA_{Mtb}$ (blues shades), $IpdB_{Mtb}$ (orange shades), and $IpdAB_{RHA1}$ (gray).

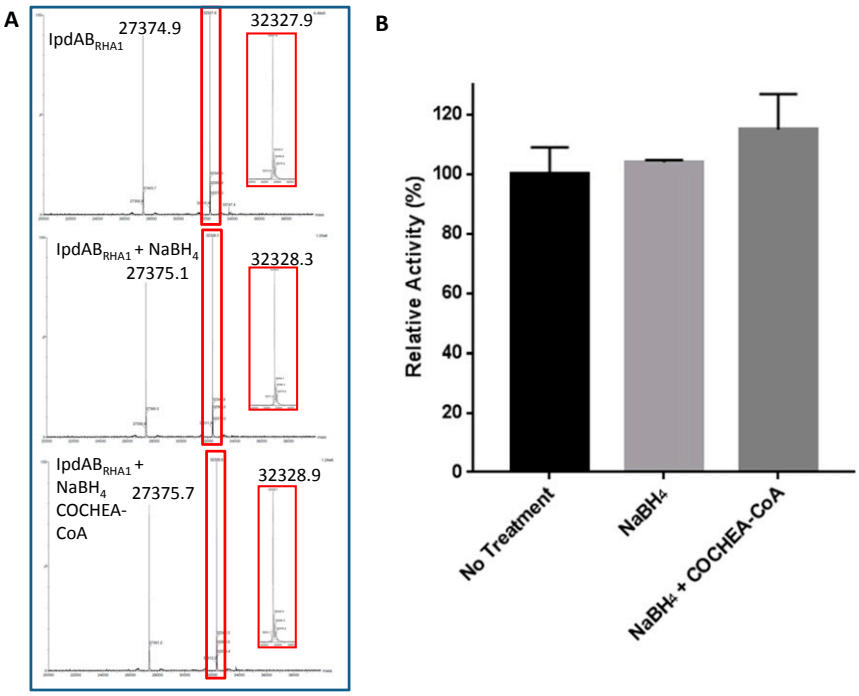


**Fig. S5.** Additional $NaBH_4$ and $^{18}O$ experimental data. (*A*) Intact protein LC-MS of $IpdAB_{RHA1}$ treated with sodium borohydride in the presence and absence of COCHEA-CoA. Shown are reconstructed masses. Red boxes indicate the species corresponding to $IpdA_{RHA1}$ where an acyl-enzyme intermediate is predicted to be identified as a mass adduct of 760–980 Da. Instrument is accurate to ±1 Da. (*B*) Treatment with sodium borohydride did not trap an intermediate. Fifty-microliter samples of IpdAB were incubated for 20 min in the presence of the indicated compounds (10 mM sodium phosphate, pH 8.0) then desalted. The specific activity of each sample was determined in the presence of 50 μM COCHEA-CoA, 150 μM CoASH, and 4 μM FadA6 in 200 μL Hepes, 1 mM $MgCl_2$, pH 7.5 ($I$ = 0.01 M) at 25 °C. Activities are reported relative to the no-treatment control. Bars indicate SD ($n$ = 3).

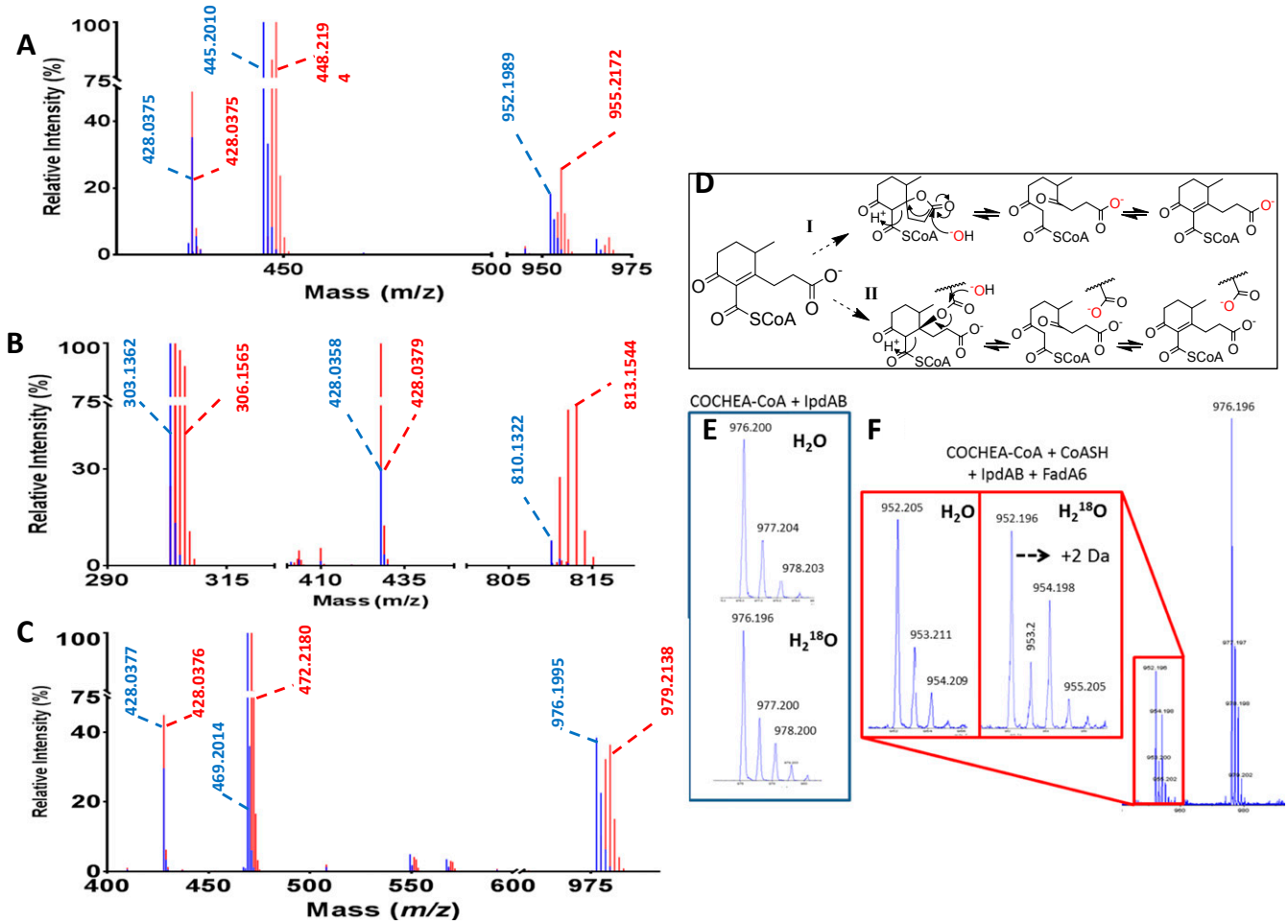


**Fig. S6.** Isotopic labeling data. LC-MS/MS spectra of MOODA-CoA (*A*) and acetyl-CoA (*B*) produced from 100 μM COCHEA-CoA in the presence of 10 μM FadA6, 2 μM IpdAB, and 125 μM CoASH incubated in 10 mM sodium phosphate, pH 8.0, prepared in water (blue) or $D_2O$ (red). Relative mass intensities are displayed. (*C*) Incubation of 100 μM COCHEA-CoA with $IpdAB_{RHA1}$ WT (red) or $E105A^A$ (blue) in the presence of $D_2O$ as described above. (*D*) Alternate mechanisms of hydrolysis of COCHEA-CoA that are not supported by experimental evidence. (*E*) The $^{18}O$ incorporation into COCHEA-CoA. LC- MS mass spectra of 100 μM COCHEA-CoA following incubation with 5 μM IpdAB (*E*) or (*F*) 2 μM IpdAB, 20 μM FadA6, and 125 μM CoASH in 10 mM sodium phosphate, pH 8.0, prepared in $H_2O$ or 97% ($^{18}O$ abundance) $H_2{}^{18}O$. Red box indicates mass spectra of MOODA-CoA.

**Table S1. Enzymes used in bioinformatic analyses**

| Enzyme name | Organism | Accession no. | Oligomer | Amino acid length | Refs. |
|---|---|---|---|---|---|
| IpdA | RHA1 | WP_011597005 | $\alpha_2\beta_2$ | 296 | 1 |
| IpdB | | WP_011597004 | | 253 | |
| IpdA | Mtb | WP_003900094 | $\alpha_2\beta_2$ | 292 | 1 |
| IpdB | | NP 218069 | | 250 | |
| IpdA | $MC^2$ 155 | WP_011730966 | $\alpha_2\beta_2$ | 295 | 1 |
| IpdB | | WP_011730967 | | 249 | |
| IpdA | *R. equi* | WP_005515561 | $\alpha_2\beta_2$ | 296 | 2 |
| IpdB | | WP_005515563 | | 249 | |
| IpdA | ACG33 | WP_066922609 | $\alpha_2\beta_2$ | 291 | 3 |
| IpdB | | WP_066917840 | | 255 | |
| IpdA | CNB2 | WP_012837471 | $\alpha_2\beta_2$ | 292 | 1 |
| IpdB | | WP_012837472 | | 256 | |
| IpdA2 | *R. equi* | CBH46238 | $\alpha_2\beta_2$ | 291 | 2 |
| IpdB2 | | WP_013414424 | | 252 | |
| $GCT_\alpha$ | *A. fermentans* | 1POI_A* | $\alpha_2\beta_2$ | 317 | 4 |
| $GCT_\beta$ | | 1POI_B* | | 260 | |
| PcaI | *P. putida* | AEJ14813 | $\alpha_2\beta_2$ | 276 | 5 |
| PcaJ | | WP_063422683 | | 213 | |
| YdiF | *E. coli* | 2AHV* | $\alpha_4$ | 531 | 6 |
| PCT | *C. propionicum* | WP_066048121 | $\alpha_4$ | 524 | |
| CitF | *C. argentinense* | WP_039636687 | —† | 517 | |
| CitC | *E. aerogenes* | WP_015368306 | —† | 508 | 7 |
| $ACT_\alpha$ | *E. coli* | 5DBN_A* | $\alpha_2\beta_2$ | 221 | |
| $ACT_\beta$ | | 5DBN_B* | | 223 | |
| ScoA | *H. pylori* | WP_001045174 | $\alpha_2\beta_2$ | 232 | |
| ScoB | | WP_015427828 | | 207 | |
| ScoA | *B. subtilis* | 3CDK_A* | $\alpha_2\beta_2$ | 232 | |
| ScoB | | 3CDK_B* | | 207 | |
| CtfA | *C. acetobutylicum* | WP_010890847 | $\alpha_2\beta_2$ | 218 | |
| CtfB | | WP_010890848 | | 221 | |
| SCT | Porcine | 3OXO* | $\alpha_4$ | 488 | 8 |

*PDB ID code provided.
†Biological assembly unknown.


1. Bergstrand LH, Cardenas E, Holert J, Van Hamme JD, Mohn WW (2016) Delineation of steroid-degrading microorganisms through comparative genomic analysis. *MBio* 7:e00166.
2. van der Geize R, Grommen AW, Hessels GI, Jacobs AA, Dijkhuizen L (2011) The steroid catabolic pathway of the intracellular pathogen *Rhodococcus equi* is important for pathogenesis and a target for vaccine development. *PLoS Pathog* 7:e1002181.
3. Yang FC, et al. (2016) Integrated multi-omics analyses reveal the biochemical mechanisms and phylogenetic relevance of anaerobic androgen biodegradation in the environment. *ISME J* 10:1967–1983.
4. Jacob U, et al. (1997) Glutaconate CoA-transferase from Acidaminococcus fermentans: The crystal structure reveals homology with other CoA-transferases. *Structure* 5:415–426.
5. Parales RE, Harwood CS (1993) Regulation of the pcaIJ genes for aromatic acid degradation in Pseudomonas putida. *J Bacteriol* 175:5829–5838.
6. Rangarajan ES, et al. (2005) Crystallographic trapping of the glutamyl-CoA thioester intermediate of family I CoA transferases. *J Biol Chem* 280:42919–42928.
7. Dimroth P, Loyal R, Eggerer H (1977) Characterization of the isolated transferase subunit of citrate lyase as a CoA-Transferase. Evidence against a covalent enzyme-substrate intermediate. *Eur J Biochem* 80:479–488.
8. Fraser ME, Hayakawa K, Brown WD (2010) Catalytic role of the conformational change in succinyl-CoA:3-oxoacid CoA transferase on binding CoA. *Biochemistry* 49:10319–10328.

**Table S2. X-ray crystallographic data collection and refinement statistics**

| Data collection and refinement | $IpdAB_{Mtb}$ WT (twinned) | $IpdAB_{Mtb}$ WT (no twin) | $IpdAB_{RHA1}$ WT | $IpdAB_{RHA1}$ E105 $^{A}$A·COCHEA-CoA | $IpdAB_{RHA1}$ WT·COCHEA-CoA |
|---|---|---|---|---|---|
| Data collection | | | | | |
| Wavelength | 0.97777 | 0.97777 | 0.97948 | 0.97874 | 1.54 |
| Resolution range | 66.88–2.1 (2.175–2.1) | 88.86–2.1 (2.175–2.1) | 48.73–1.70 (1.76–1.70) | 47.94–1.40 (1.45–1.40) | 48.02–1.60 (1.66–1.60) |
| Space group | P $2_1$1 | P $2_1$1 | P $4_3$$2_1$2 | P $4_3$$2_1$2 | P $4_3$$2_1$2 |
| Unit cell, Å, Å, Å, °, °, ° | 66.8779 133.823 118.845 90 90.2304 90 | 66.8779 133.823 118.845 90 90.2304 90 | 68.91 68.91 241.37 90 90 90 | 69.17 69.17 241.87 90 90 90 | 69.29 69.29 241.86 90 90 90 |
| Total reflections | 456,639 (37,871) | 456,641 (37,875) | 522,304 (51,305) | 819,431 (75,359) | 837,439 (27,240) |
| Unique reflections | 119,966 (10,849) | 119,967 (10,850) | 65,026 (6,374) | 116,083 (11,331) | 77,704 (6,844) |
| Multiplicity | 3.8 (3.5) | 3.8 (3.5) | 8.0 (8.0) | 7.1 (6.7) | 10.8 (4.0) |
| Completeness, % | 98.60 (89.74) | 98.60 (89.74) | 1.00 (1.00) | 1.00 (0.99) | 0.99 (0.89) |
| Mean I/sigma (I) | 11.66 (5.33) | 11.66 (5.33) | 16.54 (2.31) | 20.62 (1.53) | 31.31 (2.13) |
| Wilson B-factor | 23.30 | 23.29 | 18.06 | 16.09 | 21.51 |
| R-merge | 0.07415 (0.1848) | 0.07415 (0.1849) | 0.09076 (0.9778) | 0.0541 (1.336) | 0.0436 (0.4061) |
| R-meas | 0.08621 (0.2177) | 0.08621 (0.2177) | 0.09699 (1.044) | 0.05838 (1.448) | 0.04563 (0.4612) |
| CC1/2 | 0.995 (0.944) | 0.995 (0.945) | 0.999 (0.818) | 1.00 (0.624) | 1.00 (0.934) |
| CC* | 0.999 (0.986) | 0.999 (0.986) | 1.00 (0.949) | 1.00 (0.877) | 1.00 (0.983) |
| Refinement | | | | | |
| Reflections used in refinement | 119,965 (10,849) | 119,966 (10,850) | 65,021 (6,374) | 116,047 (11,327) | 77,599 (6,823) |
| Reflections used for R-free | 5,983 (493) | 5,983 (493) | 3,311 (347) | 5,804 (567) | 3,838 (357) |
| R-work | 0.1462 (0.2567) | 0.2411 (0.2351) | 0.1611 (0.2257) | 0.1504 (0.2756) | 0.1610 (0.4059) |
| R-free | 0.1772 (0.2891) | 0.2741 (0.2867) | 0.1916 (0.2508) | 0.1716 (0.2766) | 0.1886 (0.3955) |
| CC(work) | 0.856 (0.807) | 0.861 (0.822) | 0.971 (0.911) | 0.978 (0.830) | 0.973 (0.903) |
| CC(free) | 0.857 (0.709) | 0.853 (0.682) | 0.962 (0.893) | 0.971 (0.776) | 0.964 (0.880) |
| No. of nonhydrogen atoms | 17,607 | 17,607 | 4,700 | 5,014 | 4,874 |
| Macromolecules | 16,612 | 16,612 | 4,148 | 4,215 | 4,183 |
| Ligands | 995 | 995 | 79 | 78 | 78 |
| Protein residues | 2,164 | 2,164 | 551 | 543 | 542 |
| RMS bonds, Å | 0.017 | 0.013 | 0.006 | 0.006 | 0.006 |
| RMS angles, ° | 1.67 | 1.49 | 0.83 | 0.92 | 0.93 |
| Ramachandran favored, % | 95.95 | 95.95 | 97 | 97 | 98 |
| Ramachandran allowed, % | 3.77 | 3.82 | 3 | 2.5 | 2.4 |
| Ramachandran outliers, % | 0.28 | 0.23 | 0 | 0 | 0 |
| Rotamer outliers, % | 1.99 | 1.23 | 0.23 | 0.45 | 0.23 |
| Clash score | 2.13 | 2.35 | 1.56 | 2.01 | 3.23 |
| Average B-factor, $Å^2$ | 26.10 | 25.33 | 23.6 | 25.4 | 27.0 |
| Macromolecules | 25.82 | 25.02 | 21.3 | 22.0 | 24.3 |
| Ligands | | | 71.7 | 66.3 | 71.9 |
| Solvent | 30.76 | 30.35 | 35.7 | 40.4 | 39.6 |
| No. of TLS groups | NA | NA | 19 | 18 | 18 |

Atomic coordinates were deposited in the PDB as WT $IpdAB_{Mtb}$ (6CON), WT $IpdAB_{RHA1}$ (6CO6), E105$^{A}$A $IpdAB_{RHA1}$:COCHEA-CoA (6COJ), and WT $IpdAB_{RHA1}$:COCHEA-CoA (6CO9). NA, not applicable; TLS, Translation/Libration/Screw.